Earthquakes and Structures, *Vol. 14, No. 2 (2018) 179-186*
DOI: https://doi.org/10.12989/eas.2018.14.2.179

The numerical study of seismic behavior of gravity retaining wall built near rock face

Hossein Taravati and Alireza Ardakani*

Department of Civil Engineering, Imam Khomeini International University, Qazvin, Iran

(Received July 14, 2017, Revised February 10, 2018, Accepted February 12, 2018)

Abstract. We present the accurate investigation the seismic behavior of the gravity retaining wall built near rock face based on numerical method. The retaining wall is a useful structure in geotechnical engineering, where the earthquake is a common phenomenon; therefore, the evaluation of the behavior of the retaining wall during an earthquake is essential. However, in all previous studies, the backfill behind the wall was usually approximated by a homogeneous region, while in contrast, in practice, in many cases retaining walls are used to support the soil pressure in, inhomogeneous, mountainous area. This suggests an accurate investigation of the problem, i.e., numerical analysis. The numerical results will be compared with some of recently proposed analytical methods to show the accuracy of the proposed method. We show that increasing the volume of the rock face yields decreasing the permanent horizontal displacement of the gravity retaining wall built near rock face. Besides, we see that the permanent horizontal displacement of the gravity retaining wall with homogenous backfill is more than permanent horizontal displacement of the gravity retaining wall case of the built near rock face in different frequency contents.

Keywords: gravity retaining wall; near rock face; seismic behavior; earthquake; numerical method

1. Introduction

The retaining wall restricts the soil to a slope, e.g., a steep or vertical slope, and bounds the soils between different elevations, usually in the areas where the landscape requires to be shaped and engineered for specific purposes, e.g., roadway overpasses. To design a retaining wall, specific information about the predicted values of the, translational and rotational, wall displacement is required Excessive displacements lead to the wall failure and cause damage to the adjacent structures. However, the reported displacement-based methods in seismic design of the retaining structures, which are mainly based on the Newmark's sliding block theory, are incapable to predict an acceptable mechanism for the lateral displacement caused by the earthquake (Newmark 1965). These methods are formed essentially based on the quasi-static method suffer from different drawbacks, i.e., ignoring the soil deformability and seismic acceleration of the backfill behind the wall. Therefore, it is necessary to develop another realistic approach.

In dynamic analysis method, the response of the structure is recorded during the earthquake, considering the actual characteristics of the soil model, input excitation to the system and the interaction between materials. This method presents various advantages, including the applied effect of the initial stresses, considering the impact of the behavioral parameters of the material in the response of the structure, ability to change the shear strength during the earthquake, and taking into account the effect of the earthquake parameters, e.g., amplitude and frequency contents. However, in some cases, the retaining walls may support the soil pressure in mountainous areas. For the sake a simplification in such a situation, the reported analytical methods consider a homogeneous and granular backfill behind the retaining walls, while in few cases the impact of the heterogeneity of the backfill evaluated by the static and quasi-dynamic methods. Therefore, to identify and design these types of structures, the investigation of the problem using more accurate techniques, e.g., numerical modeling by time history dynamic analyses, being useful and essential.

In the last decade, numerous numerical and experimental studies have been performed on behavior of the retaining walls (Aminpoor and Ghanbari 2014, Azarafza *et al*. 2017, Bray *et al*. 2010, Cakir 2014, Cakir 2017, Ghosh and Sharma 2012, Ismeik and Shaqour 2015, Ouria *et al*. 2016, Temur and Bekdas 2016). Clough and Duncan (1971) employed the finite element method to study the static behavior of the retaining walls including the interface effects between the structure and the surrounding soil. Nakamura (2006) performed a series of dynamic centrifuge experiments to study the seismic behavior of the gravity retaining walls, and investigated the accuracy of the Mononobe-Okabe assumptions. He presented great insights into the seismic behavior of the gravity wall-backfill system. Tiznado (2011), Tiznado and Rodriguez (2011) numerically studied the lateral displacement of the gravity retaining wall located on the granular soil. They used the elasto-plastic model of HSS for the soil behavior. Athanasopoulos *et al*. (2013) evaluated phasing issue in the seismic response of the gravity retaining walls by a finite element study. For the first time, Frydman and Keissar

*Corresponding author, Assistant Professor
E-mail: a.ardakani@eng.ikiu.ac.ir

ISSN: 2092-7614 (Print), 2092-7622 (Online)

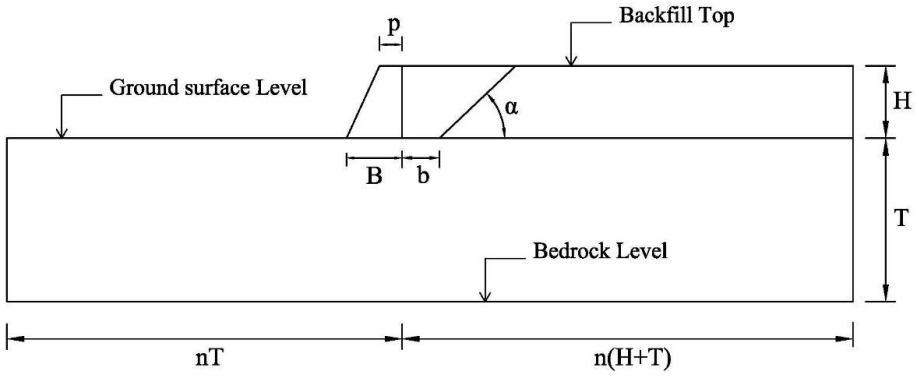

Fig. 1 Schematic view of the performed numerical modeling

(1987) studied a retaining wall built near rock face, and carried out their study by modeling in a centrifuge. In addition to the modeling of the aluminum wall, they used a disk-like tool and wooden block for the simulation of the backfill and rock face, where a Load cell is installed on the device to record the results and measure the active pressure on the soil. Considering the calibrated device, they started analysis and evaluated the pressure change from rest to active condition. Ardakani *et al*. (2018) showed that behaviors of geotechnical structures are different under monotonic and cyclic loading.

2. Effect of the frequency content on the seismic behavioral of retaining wall

The spectrum of an earthquake provides the amplitude of the waves for different frequencies. In fact, the different in frequency content of two earthquakes with equal energy and peak ground acceleration causes the different in the response of the structure (Gazetas *et al*. 2004, Cakir 2013). Earthquake frequency contents appear in the acceleration response spectrum, i.e., reflectance spectrum, or Fourier spectrum. Hatami and Bathurst (2001), Varnier and Hatami (2011) studied the reinforced soil retaining walls and showed that the input acceleration with equal peak ground acceleration can results different response of wall and seismic response of reinforced soil retaining walls is function of several parameters including their intensity and their frequency contents. Tufan (2013) investigated the effect of the frequency content on the seismic behavior of cantilever retaining wall and showed that frequency content may represent one of the most important parameters that should be considered in the seismic design of this structure.

3. Numerical modelling

3.1 Principles

This Section presents the numerical results and compares them with those of a recently proposed analytical method. Given the absence of the water table, the soil mass balance is applied only with in-situ stresses.The Soil element used in this study is a six-node triangular element

Table 1 Material properties in numerical modeling

Type of model	Homogenous backfill		Near rock face
Area	Backfill	Foundation	Fackfill
Φ (°)	37	40	37
C (kPa)	0	0	0
γ (kN/m^3)	17	18	17
E_{50}^{ref} (MPa)	40	45	40
E_{oed}^{ref} (MPa)	40	45	40
E_{ur}^{ref} (MPa)	120	135	120
$\gamma_{0.7}$	0.0002	0.0002	0.0002
G_0^{ref} (kPa)	95700	98200	95700

with three-point Gaussian for each element, and the interface elements are placed between the wall and backfill and between the rock face and backfill. Besides, the strength reduction factor of the interface element, R_{inter}=0.7, represents the ratio of the interface strength to the shear strength of the surrounding soils. The hardening soil model with small-strain stiffness, HS_{small} model, is chosen to represent the soil stress-strain behavior. We assume a linear elastic behavior for the wall and rock face, with a Poisson's ratio of 0.2, unit weight of 24 kn/m^3 and use a high enough Young's modulus (E=2×10^7 for rock face and E=2.5×10^7 for reinforced concrete wall) to simulate a rigid structure. Characteristics of material assigned to the models listed in Tables 1. Fig. 1 illustrates the schematic view of the performed numerical modeling. It should be noted that n=3 was considered in modeling shown in Fig. 1. Figs. 2 and 3 indicate the finite element meshes for the two models "with homogenous backfill" and "near rock face", respectively. Table 2 presents the dimensions of the analytical models in PLAXIS code. The appropriate selection of the elements dimensions in a numerical analysis is very important duo to its impact on the accuracy of the results. The application of small elements either requires high-performance computing systems or yields a significant increase in the analysis time. On the other hand, the application of large elements reduces the accuracy of the analysis. In general, to properly transfer the dynamic waves in the network of the model elements, an approximate formula for dimension of the elements, $\Delta l_{\max}$, is as follows

$$\Delta l_{\max} = \frac{\lambda_{\min}}{8} \sim \frac{\lambda_{\min}}{10} \quad (1)$$

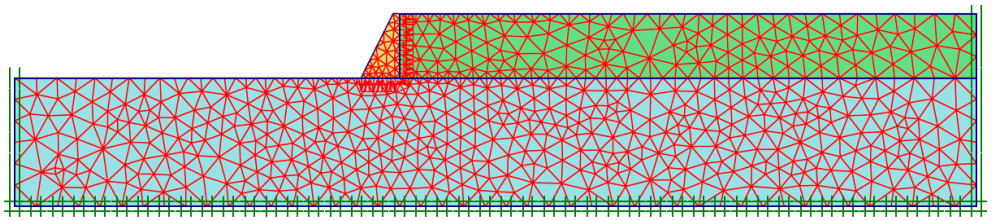

Fig. 2 Finite element mesh for the homogenous backfill

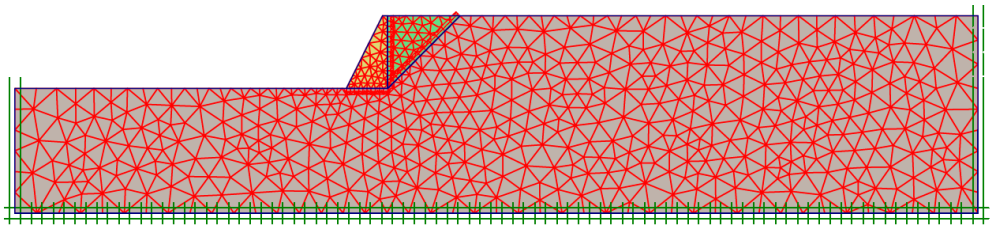

Fig. 3 Finite element mesh for the near rock face

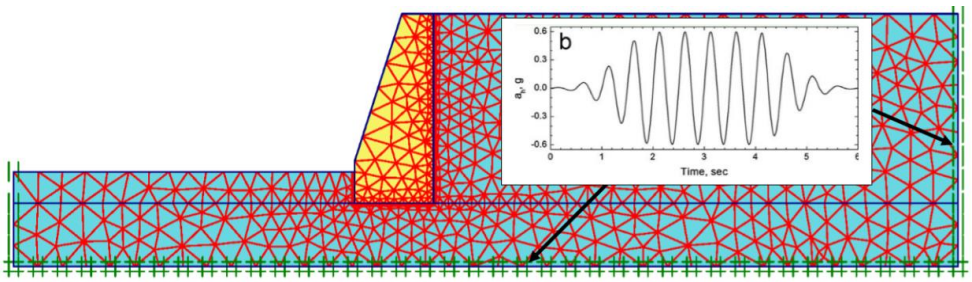

Fig. 4 The model proposed by Nakamura (2006)

Table 2 Dimensions of the analytical models

Type of model	Homogenous backfill	Near rock face
Height of wall, H (m)	5	7
Height of foundation, T (m)	10	10
Bottom width of wall, B (m)	3	4
Top width of wall, P (m)	0.5	0.5

With

$$\lambda_{\min} = \frac{V}{f_{\max}} \tag{2}$$

Where $\lambda_{\min}$ is the minimum wavelength of the earthquake spectrum, V and $f_{\max}$ are the velocity of the waves in model and the maximum frequency of the earthquake, respectively. In this research, in addition to this criterion, mesh sizes are selected based on initial analysis to ensure the accuracy achieved. Also we employed the Rheyleight damping for modeling, representing a common mechanical damping, used in the dynamic analyses. The Rheyleight damping damps the natural oscillatory modes of the system in the analyses of the structures. Therefore, equations may be expressed in matrix form as

$$c = \alpha.M + \beta.K \tag{3}$$

Where C represents the damping matrix, M and K denote the mass and stiffness matrices, respectively. α and β are the mass and stiffness coefficients, respectively. The parameters α and β can be derived from Eq. (4).

Table 3 Material properties in the model built by Nakamura (2006)

Parameter	γ (kN/m^3)	E (MPa)	ν	Φ (°)	C (kPa)
Value	15	40	0.33	37	2

$$\begin{Bmatrix}\alpha\\ \beta\end{Bmatrix} = \frac{2\xi}{\omega_n+\omega_m}\begin{Bmatrix}\omega_n\omega_m\\ 1\end{Bmatrix} \tag{4}$$

With ω_n and ω_m being the natural rotational frequencies corresponding to the main, first and second, modes and ξ indicates the damping ratio, set to 5% for this study.

We use the centrifuge model, case 18, proposed by Nakamura (2006), where, for the sake of comparison, the same materials and harmonic acceleration are considered in both analytical and numerical models. Fig. 4 shows the model proposed by Nakamura (2006), which is used for the verification. Table 3 lists material properties assigned in the model of Nakamura (2006). Fig. 5 compares the numerical results in this study and those achieved using the analytical method of Nakamura (test #18). We see that there is a good agreement between these two results.

3.2 The HS_{small} model

The HS_{small} model is an elastoplastic constitutive model, where shear hardening, due to plastic strains during the primary deviatoric loading is modeled by a yield surface that may isotropically expand up to the Mohr-Coulomb failure criterion (Ardakani *et al*. 2014, Benz 2006). A yield

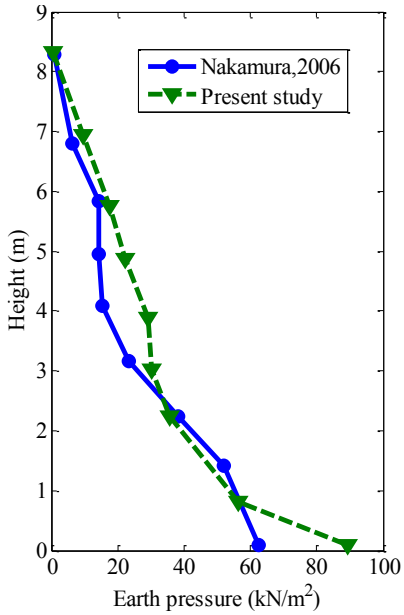

Fig. 5 Comparison seismic pressures of soil along the wall between the analytical method (Nakamura 2006) and numerical results in the present study

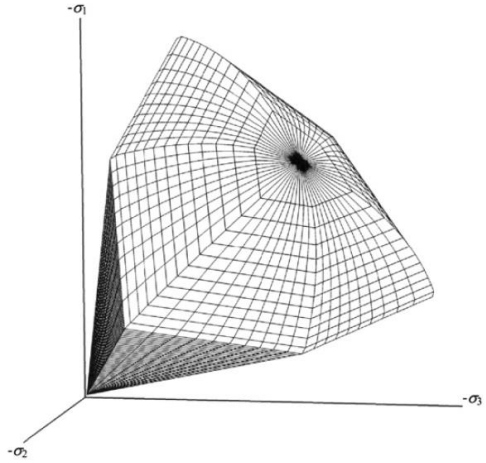

Fig. 6 Yield surface in the principal stress space for cohesionless soil (Plaxis 2D. Reference Manual 2002)

cap is introduced for the model compression hardening, i.e. plastic strains due to primary compression in oedometer loading and isotropic loading (Fig. 6). This model uses a non-associated flow rule for shear hardening and an associated flow rule for the compression hardening. Negative and positive values are used for the compressive and tensile stresses, respectively.

In the particular case of standard triaxial-test loading conditions, the model leads to the well-known Duncan and Chang hyperbolic stress-strain relationship (Duncan and Chang 1970). The soil stiffness for primary loading is modeled using the secant E_{50} defined at 50% ultimate strength (Fig. 7). This modulus is given by

$$E_{50}= E_{50}^{ref}\left(\frac{c\cos\varphi - \sigma'_3 \sin\varphi}{c\cos\varphi + p^{ref}\sin\varphi}\right)^m \quad (5)$$

where σ'_3 is the effective confining pressure, crepresents

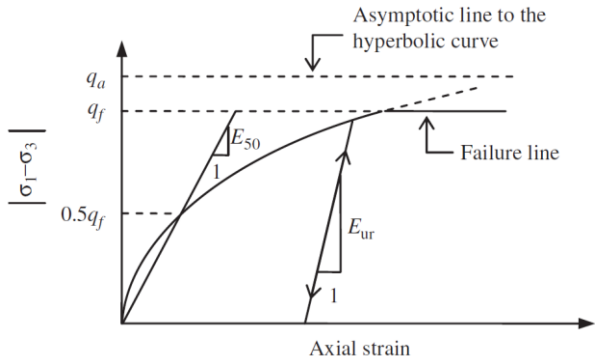

Fig. 7 Hyperbolic stress-strain relation for standard compression triaxial test (Plaxis 2D. Reference Manual, 2002)

the cohesion, ϕ being the peak friction angle, E_{50}^{ref} denotes the secant modulus for the reference confining pressure p^{ref} (usually equal to 100 KN/m^2), and $m$is the constant dimensionless number.

The shear hardening flow rule is expressed as

$$\varepsilon_v^{\rho}= \sin\psi_m\, \dot{\gamma}_{\rho} \quad (6)$$

$$\begin{pmatrix} \text{For } \sin\varphi_m < \frac{3}{4}\sin\varphi & \psi_m=0 & \\ \text{For } \sin\varphi_m \geq \frac{3}{4}\sin\varphi & \text{and } \psi>0 & \sin\psi_m = \max\left(\frac{\sin\varphi_m - \sin\varphi_{cv}}{1-\sin\varphi_m \sin\varphi_{cv}}, 0\right) \\ \text{For } \sin\varphi_m \geq \frac{3}{4}\sin\varphi & \text{and } \psi=0 & \psi_m=\psi \end{pmatrix} \quad (7)$$

$$\sin\varphi_m = \frac{(\sigma'_1 - \sigma'_3)}{(\sigma'_1 + \sigma'_3 - 2\cot\varphi)} \quad (8)$$

The angle of dilatancy at failure, ψ, is expressed in terms of the peak friction angle, ψ, as

$$\sin\psi = \frac{(\sin\varphi - \sin\varphi_{cv})}{(1-\sin\varphi \sin\varphi_{cv})} \quad (9)$$

The critical state angle, ϕ_{cv} is automatically computed from Eq. (9). Therefore, plaxis users do not require specifying this angle. In unloading-reloading cycles, the nonlinear shear-modulus reduction with shear-strain amplitude is considered using the following modified Hardin and Drnevich hyperbolic relationship.

$$\frac{G}{G_0} = \frac{1}{1+0.385\left[\frac{\gamma}{\gamma_{0.7}}\right]} \quad (10)$$

where G_0 represents the shear modulus at very small shear strains ($\gamma<10^{-6}$), G is the secant shear modulus corresponding to the shear strain amplitude γ, and $\gamma_{0.7}$ being the shear strain value at which the secant shear modulus G is reduced to about 70% of G_0.

In the HS_{small} model, the shear-modulus reduction curve is bounded by a certain lower limit as shown in Fig. 8. We consider the Masing's rule for modeling the soil hysteretic behavior in the unloading-reloading cycles. The formulation of this model has been developed mainly for geotechnical applications where the small cycles of the shear strains take

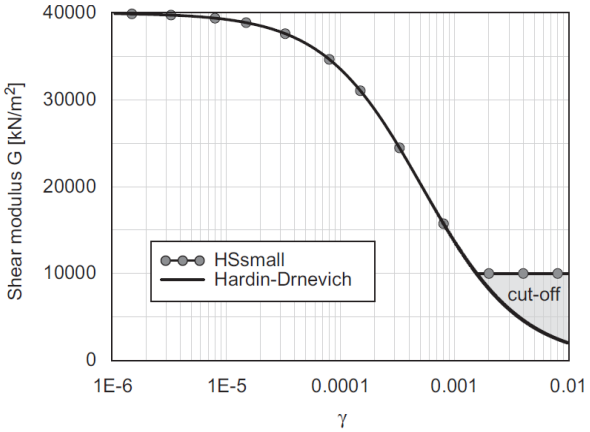

Fig. 8 Cut-off of the shear-modulus degradation curve in the HS_{small} model (Plaxis 2D. Reference Manual 2002)

place, i.e., when shear strains are lower than 0.001, approximately. The Plaxis manual and Benz *et al*. (2009) provide a more detailed description of the HS_{small} model. The following parameters are required by the model.

c: effective cohesion

ϕ: effective friction angle at peak strength

ψ: angle of dilatancy at failure

v_{ur}: Poisson's ratio for unloading-reloading, where the default value is 0.2

K_0: coefficient of the earth pressure at rest, where K_0=1-sinϕ for the normally consolidated sands

m: dimensionless E_{50}-modulus exponent

R_f: failure ratio defined as q_f/q_a (Fig. 7) (The default value is 0.9)

E_{50}^{ref}: E_{50}-modulus at the reference confining pressure p^{ref}

E_{oed}^{ref}: tangent oedometer modulus at the reference pressure (the default relation is: $E_{oed}^{ref} = E_{50}^{ref}$)

E_{ur}^{ref}: Young's modulus for unloading-reloading conditions, at the reference confining pressure (the default relation is: $E_{ur}^{ref} = 3\,E_{50}^{ref}$

G_0^{ref}: dynamic shear modulus at very small strains, at the reference pressure

$\gamma_{0.7}$: shear strain value at which the secant shear modulus G is reduced to about 70% of G_0.

4. Backfill width and rock face inclination impacts on the seismic behavior of the gravity retaining wall

This section evaluates the effect of two geometrical parameters, i.e. the inclination of rock face and the width of backfill, on the seismic behavior of gravity retaining wall built near rock face. The inclination of the rock face reads 30°,45°,60° and 75° (α in Fig. 1) and the width of backfill reads 0, 1 and 2 meter. The applied record of the numerical model is the horizontal component of the Tabas earthquake acceleration, Boshrooy station, set to 0.3 g. It should be noted that in all analyses, we consider the point at the front of wall in mid-high considered as the horizontal displacement of wall.

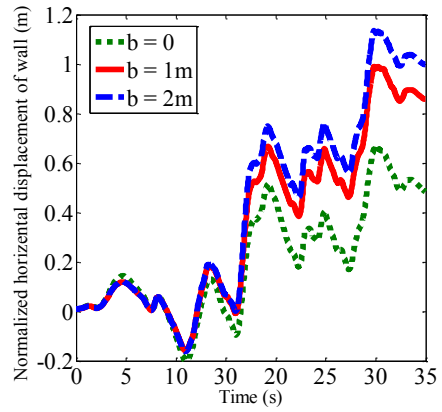

(a) α=30°

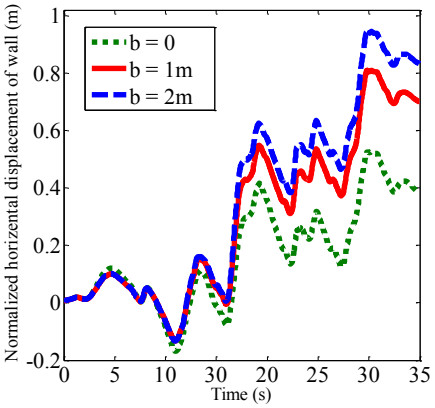

(b) α=45°

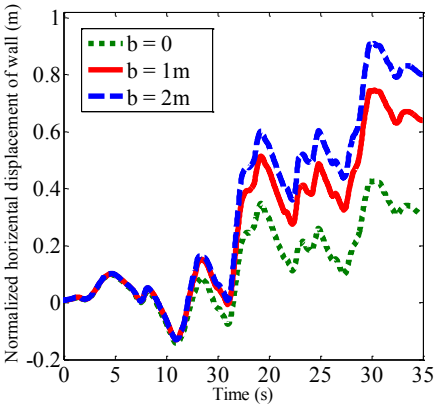

(c) α=60°

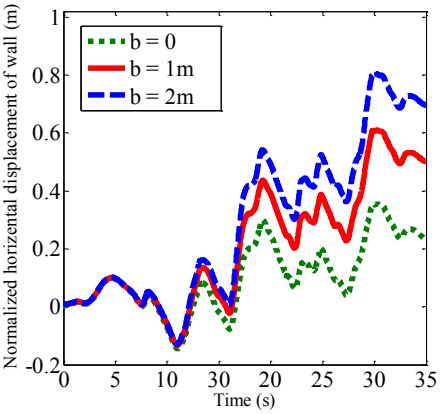

(d) α=75°

Fig. 9 Horizontal displacement of the wall for different widths of backfill

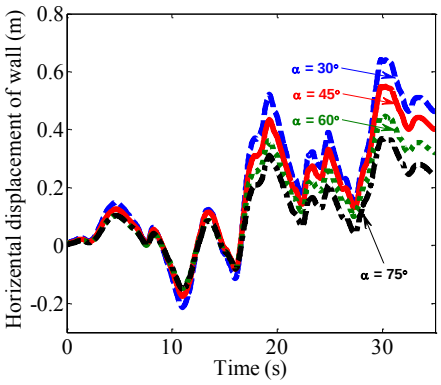

(a) b=0.0 m

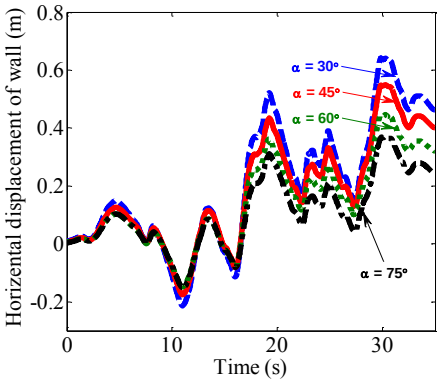

(b) b=1.0 m

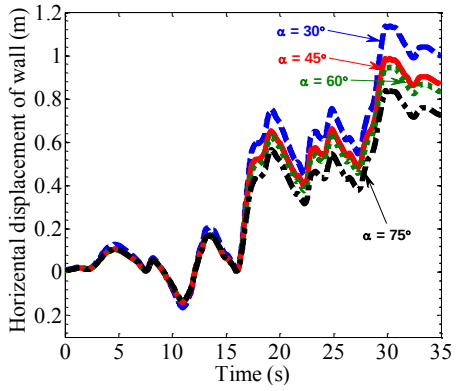

(c) b=2.0 m

Fig. 10 Horizontal displacement of the wall for different inclinations of rock face

4.1 Backfill width effect on the seismic behavior of gravity retaining wall

To evaluate the impact of the width of the backfill on the seismic behavior of gravity retaining wall built near rock face, we consider the widths equal to 0, 1and 2 meter. In constant, inclinations of the rock face, that is 30°, 45°, 60° and 75°, the effect of the width of the backfill on horizontal displacement of the wall, at the point of front of the wall in mid-high, recorded.

Fig. 9 plots the horizontal displacement of the wall for different backfill widths, i.e., α= 30°, 45°, 60° and 75°.

As can be seen in Fig. 9, in all cases increasing the width of backfill (parameter b in Fig. 1) results in increase in (maximum and permanent) horizontal displacement of wall (at the point of front of wall in mid-high).

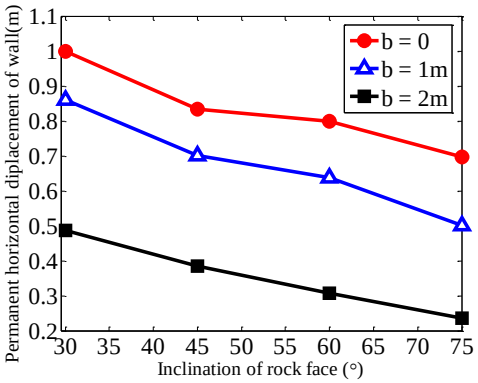

Fig. 11 The Effect of the rock face inclination and backfill width on the permanent displacement of gravity retaining wall

4.2 Evaluation of the effect of rock face inclination on seismic behavior of gravity retaining wall

To evaluate the impact of the rock face inclination on the seismic behavior of gravity retaining wall built near rock face, we choose various inclinations, i.e., 30°, 45°, 60° and 75°. Fig. 10 shows the results for the constant backfill widths of 0, 1 and 2 meter. Fig. 11 plots the effect of the rock face inclination and width of the backfill on the permanent horizontal displacement of the wall.

Fig. 10 reveals that, in all cases, increasing the inclination of the rock face leads to decreasing the permanent horizontal displacement of the wall, at the point of front of wall in mid-high. The results from Fig. 11 show that increasing the inclination of the rock face and decreasing the width of the backfill, that result in increase in the volume of the rock face, yields decreasing the permanent horizontal displacement of the wall. Moreover, in case of α=30° and b=2 m, i.e., the maximum volume of the backfill or in other words the minimum volume of the rock face, the permanent horizontal displacement of the wall is 4.24 times of the case of α=75° and b=0, where the minimum volume of the backfill or in other word maximum volume of rock face. Besides, changing the width of the backfill from 0 to 1 m affects more on the permanent horizontal displacement of the wall, increasing by 93%, than changing the width of the backfill from 1 to 2.0 m, which yields increasing by 27%.

5. Rock face presence effect on the seismic behavior of retaining wall for different frequency contents

Tso *et al*. (1992) showed that the ratio of PGA/PGV represents the relative frequency content of the ground motion. Therefore, a good indicator for the frequency content is the ratio of PGA which is expressed in units g to PGV expressed in units m/s. Earthquake records may be classified into three groups according to the frequency content ratio, including the high PGA/PGV ratio when PGA/PGV=1.2, the intermediate PGA/PGV ratio when

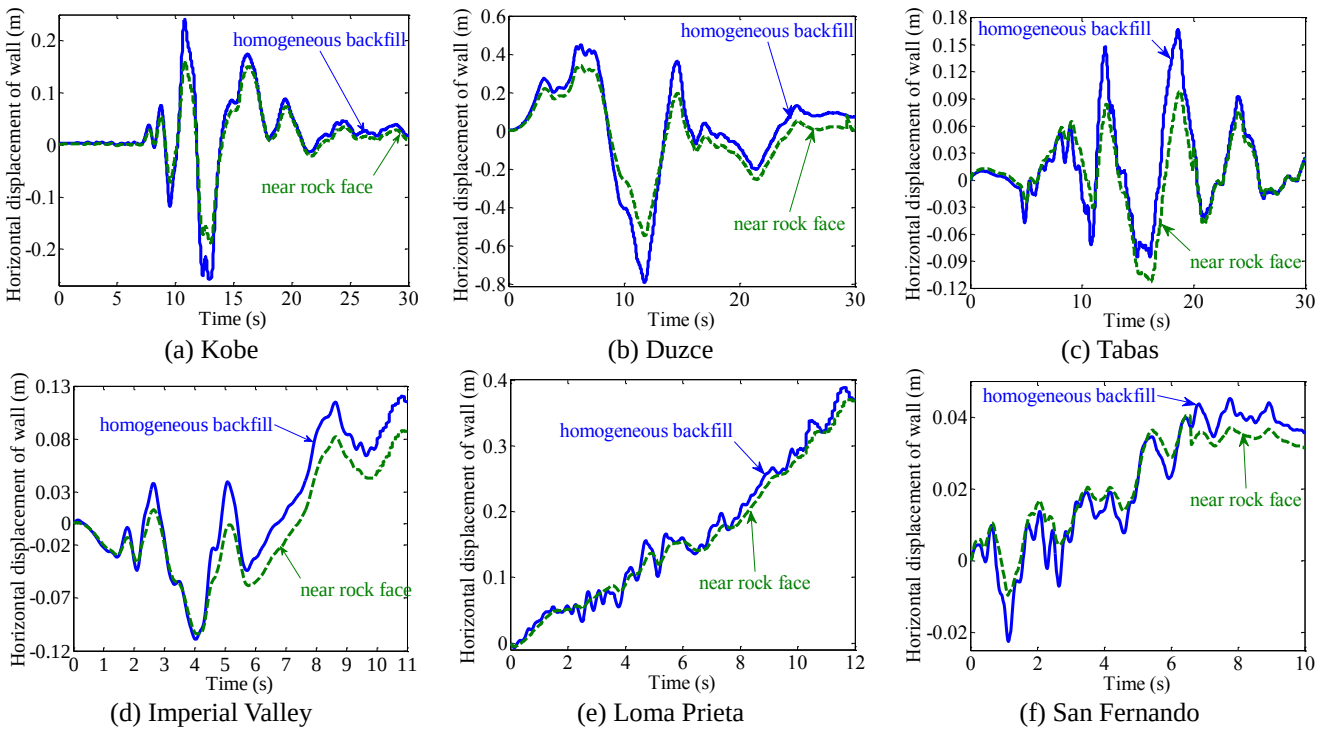

Fig. 12 Horizontal displacement of the wall normalized to PGA=0.3 g under different records

Table 4 Characteristics of the applied records to the models

Earthquake	Station	PGA/PGV (1/s)	PGA/PGV (category)
Kobe	Takatori	0.4	Low
Duzce	Sakarya	0.43	
Tabas	Tabas	0.857	Intermediate
Imperial valley	USGS Station 117	0.986	
Loma Prieta	47125 Capitola	1.26	High
San Fernando	Santa Anita Dam	2.57	

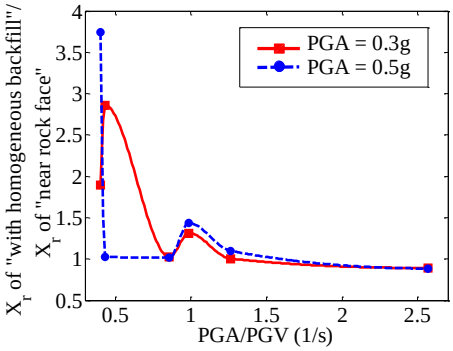

Fig. 13 The ratio of the permanent displacement of the wall with homogeneous backfill to the permanent displacement of the wall near rock face in different values of PGA and PGA/PGV. X_r=Permanent horizontal displacement of wall

PGA/PGV between 1.2 and 0.8, and the low PGA/PGV ratio when PGA/PGV=0.8. We scaled all actual records to a specific scale, to evaluate the effect of the frequency content and the independency of the numerical analysis to peak ground acceleration. Moreover, for separately evaluation of the impact of the peak ground acceleration, two different values were considered, i.e., 0.3 and 0.5 g. The aims are two, first, evaluate the effect of the frequency content of the input excitation on the permanent horizontal displacement of the wall in two cases of "homogeneous backfill" and "near rock face". And second, to observe the effect of the presence of the rock face on the permanent horizontal displacement of the wall for the input excitations with equal peak ground acceleration and different frequency contents. It should be noted that, models shown in Figs. 2 and 3 used for modeling and same material properties were assigned. The inclination of the rock face, parameter α in Fig. 6, is set to 45°. Table 4 shows the characteristics of the records applied to the models. Fig. 12 plots the impact of the rock face on the seismic behavior of retaining wall for various frequency contents. As we see from this figure, in all cases, the permanent horizontal displacement of the wall in condition of "homogeneous backfill" is more than the permanent horizontal displacement of wall in condition of "near rock face" in different frequency contents.

As can be seen in Fig. 12, in all cases, the permanent horizontal displacement of wall in condition of "homogeneous backfill" is more than the permanent horizontal displacement of wall in condition of "near rock face" in different frequency contents.

Fig. 13 shows the ratio of the permanent horizontal displacement of the wall with homogeneous backfill to the permanent horizontal displacement of wall near rock face in different values of PGA and PGA/PGV. The ratio of permanent horizontal displacement of "wall with homogeneous backfill" to the permanent horizontal displacement of "wall near rock face" is maximum 3.75 and minimum 1 in different PGA and PGA/PGV. Moreover, difference between the permanent horizontal displacement of wall in two cases of "with homogeneous backfill" and

"near rock face" is remarkable in low ratios of PGA/PGV and in intermediate ratios and high ratios of PGA/PGV this difference is negligible.

6. Conclusions

We presented the numerical results for the investigations of the seismic behavior of the gravity retaining wall built near rock face. It is shown that increasing the inclination of the rock face and decreasing the width of the backfill, i.e. increasing the volume of the rock face, leads to decreasing the permanent horizontal displacement of the wall. Besides, considering the case α=30° and b=2 m, i.e., the maximum volume of the backfill or in other words minimum volume of the rock face, the permanent horizontal displacement of the wall becomes 4.24 times of the case of α=75° and b=0, i.e., minimum volume of the backfill or in other word maximum volume of the rock face. Moreover, changing the width of the backfill from 0 to 1 m affects more the permanent horizontal displacement of the wall, i.e., increasing 93%, than changing the width of the backfill from 1m to 2 m, providing 27% increase. In all cases, the permanent horizontal displacement in the case of "wall with homogeneous backfill" is more than the permanent horizontal displacement for the case of "wall near rock face" in different frequency contents. As a result, the ratio of the permanent horizontal displacement of the "wall with homogeneous backfill" to the permanent horizontal displacement of the "wall near rock face" is maximum 3.75 and minimum 1 for different PGA and PGA/PGV. Moreover, difference between the permanent horizontal displacement of the wall in two cases of "with homogeneous backfill" and "near rock face" is remarkable in low ratios of PGA/PGV, while for the intermediate and high ratios of PGA/PGV this difference is negligible.

References

Aminpoor, M. and Ghanbari, A. (2014), "Design charts for yield acceleration and seismic displacement of retaining walls with surcharge through limit analysis", *Struct. Eng. Mech.*, **52**(6), 1225-1256.

Ardakani, A., Bayat, M. and Javanmard, M. (2014), "Numerical modeling of soil nail walls considering Mohr Coulomb, hardening soil and hardening soil with small-strain stiffness effect models", *Geomech. Eng.*, **6**(4), 391-401.

Ardakani, A., Gholampoor, N., Bayat, M. and Bayat, M. (2018), "Evaluation of monotonic and cyclic behaviour of geotextile encased stone columns", *Struct. Eng. Mech.*, **65**(1), 81-89.

Athanasopoulos-Zekkos, A., Vlachakis, V. S. and Athanasopoulos, G.A. (2013), "Phasing issues in the seismic response of yielding, gravity-type earth retaining walls-Overview and results from a FEM study", *Soil Dyn. Earthq. Eng.*, **55**, 59-70.

Azarafza, M., Feizi-Derakhshi, M. and Azarafza M. (2017), "Computer modeling of crack propagation in concrete retaining walls: A case study", *Comput. Concrete*, **19**(5), 509-514.

Benz, T. (2006), "Small-strain stiffness of soils and its numerical consequences", PhD Thesis, University Stuttgart.

Benz, T., Vermeer, P.A. and Schwab, R.A. (2009), "Small-strain overlay model", *Int. J. Numer. Anal. Meter.*, **33**(1), 25-44.

Bray, I., Travasarou, T. and Zupan, J. (2010), "Seismic displacement design of earth retaining structures", *ASCE GSP*, **208**, 638-655.

Cakir, T. (2013), "Evaluation of the effect of earthquake frequency content on seismic behavior of cantilever retaining wall including soil-structure interaction", *Soil Dyn. Earthq. Eng*, **45**, 96-112.

Cakir, T. (2014), "Backfill and subsoil interaction effects on seismic behavior of a cantilever wall", *Geomech. Eng.*, **6**(2), 601-619.

Cakir, T. (2017), "Assessment of effect of material properties on seismic response of a cantilever wall", *Geomech. Eng.*, **13**(4), 601-619.

Clough, G.W. and Duncan, J.M. (1971), "Finite element analysis of retaining wall behavior", *J. Soil Mech. Found. Div.*, ASCE, **97**(12), 1657-1673.

Duncan, J.M. and Chang, C.Y. (1970), "Nonlinear analysis of stress and strain in soils", *J. Soil Mech. Found. Div.*, ASCE, **96**(5), 1629-1653.

Frydman, S. and Keissar, I. (1987), "Earth pressure on retaining walls near rock faces", *J. Geotech. Eng.*, ASCE, **113**(6), 586-599.

Gazetas, G., Psarropoulos, P.N., Anastasopoulos, L. and Gerolymos, N. (2004). "Seismic behavior of flexible retaining system subjected to short-duration moderately strong excitation", *Soil Dyn. Earthq. Eng.*, **24**, 537-550.

Ghosh, S. and Sharma, R.P. (2012), "Seismic active earth pressure on the back of battered retaining wall supporting inclined backfill", *Int. J. Geomech.*, **12**(1), 54-63.

Hardin, B.O. and Drnevich, V.P. (1972), "Shear modulus and damping in soils: design equations and curves", *J. Soil Mech. Found. Div.*, ASCE, **98**, 667-692.

Hatami, K. and Bathurst, R.J. (2001), "Investigation of response of reinforced soil retaining walls", *Proceeding of the 4th International Conference On Recent Advances in Geotechnical Engineering and Soil Dynamic and Symposium In Honor of Professor W.D Liam Finn*, San Diego, California, USA.

Ismeik, M. and Shaqour, F. (2015), "Seismic lateral earth pressure analysis of retaining walls", *Geomech. Eng.*, **8**(4), 523-540.

Jesmani, M., Kamalzare, M. and Bahrami Sarbandi, B. (2016), "Seismic response of geosynthetic reinforced retaining walls", *Geomech. Eng.*, **10**(5), 635-655.

Nakamura, S. (2006), "Re-examination of Mononobe-Okabe theory of gravity retaining walls using centrifuge model tests", *Soils Found.*, **46**(2), 135-146.

Newmark, K.M. (1965), "Effect of earthquakes on dams and embankments", *Geotechnique*, **15**(2), 139-160.

Ouria, A., Toufigh, V., Desai, C., Toufigh, V. and Saadatmanesh, H. (2016), "Finite element analysis of a CFRP reinforced retaining wall", *Geomech. Eng.*, **10**(6), 757-774.

Plaxis 2D (2002), Reference Manual, Version 8.

Temor, R. and Bekdas, G. (2016), "Teaching learning-based optimization for design of cantilever retaining walls", *Struct. Eng. Mech.*, **57**(4), 763-783.

Tiznado, J.C. and Rodriguez-Roa, F. (2011), "Seismic lateral movement prediction for gravity retaining walls on granular soils", *Soil Dyn. Earthq. Eng.*, **31**(3), 391-400.

Tso, W., Zhu, T. and Heidebrecht, A. (1992), "Engineering implications of ground motion A/V ratio", *Soil Dyn. Earthq. Eng.*, **11**(3), 133-144.

Varnier, J. and Hatami, K. (2011), "Seismic response of reinforced soil walls: Is PGA-based design adequate?", Geo *Risk*, ASCE, 336-343.

Wu, Y. and Prakash, S. (2011), "Design charts for retaining walls in seismic areas", *ASCE GSP*, **199**, 2973-2981.

AT